

**This is an electronic reprint of the original article.  
This reprint *may differ* from the original in pagination and typographic detail.**

**Author(s):** Harjupatana, Tero; Alaraudanjoki, Jarno; Kataja, Markku

**Title:** X-ray tomographic method for measuring 3D deformation and liquid content in swelling materials

**Year:** 2015

**Version:**

**Please cite the original version:**

Harjupatana, T., Alaraudanjoki, J., & Kataja, M. (2015). X-ray tomographic method for measuring 3D deformation and liquid content in swelling materials. In R. Kouhia, J. Mäkinen, S. Pajunen, & T. Saksala (Eds.), *Proceedings of the XII Finnish Mechanics Days : Suomen XXII mekaniikkapäivien esietlmät* (pp. 222-227). Rakenteiden mekaniikan seura.

All material supplied via JYX is protected by copyright and other intellectual property rights, and duplication or sale of all or part of any of the repository collections is not permitted, except that material may be duplicated by you for your research use or educational purposes in electronic or print form. You must obtain permission for any other use. Electronic or print copies may not be offered, whether for sale or otherwise to anyone who is not an authorised user.

# X-ray tomographic method for measuring 3D deformation and liquid content in swelling materials

Tero Harjupatana<sup>1</sup>, Jarno Alaraudanjoki<sup>1</sup> ja Markku Kataja<sup>1</sup>

<sup>(1)</sup>University of Jyväskylä, Department of Physics, tero.t.harjupatana@jyu.fi

**Summary.** A non-invasive method for measuring the three-dimensional displacement field and liquid content distribution in a wetting and swelling material using X-ray tomographic imaging is introduced. The method is demonstrated here in monitoring the evolution of 3D deformation and water content distributions in cylindrical samples of swelling clay material wetted in a constant total volume. The measurements were carried out using a high-resolution microtomographic device (SkyScan 1172) and image voxel size 24  $\mu\text{m}$ . The results obtained are repeatable and appear qualitatively correct and plausible. They are useful e.g. in validating models involving transport of water and the resulting deformation of swelling materials. The method is potentially applicable also in other materials and processes involving liquid transport and deformation.

*Key words:* X-ray tomography, liquid content, liquid transport, deformation, bentonite, swelling, wetting.

## Introduction

The dynamics of liquid transport and deformation in processes involving wetting or drying of solid materials such as soils, building materials, foods and various biological materials [1, 2, 3, 4] can be quite complicated. Theoretical approaches based on first principles towards modelling these processes tend to become tedious, and phenomenological input is often required. Measuring the total liquid content and the global deformation of a wetting/drying material sample is rather straightforward by conventional gravimetric and morphological methods [5, 6]. At least rough local information can be obtained by destructive segmenting of the sample. Various modalities of tomography and other non-destructive methods have been used for measuring the local three-dimensional liquid content distribution [7, 8, 9, 10] or the local deformation of material samples in various mechanical conditions [11, 12]. However, few efforts appears to have been made towards simultaneous non-destructive measurement of the evolution of both the liquid content and the local deformation field of a material sample during wetting or drying process. Availability of such a measurement method would be potentially useful for experimental research of processes involving liquid transport and the resulting deformation, and for development and validation of theoretical models of such processes.

In this work, we introduce a method based on X-ray microtomography for non-destructive simultaneous measurement of three dimensional distribution of local liquid content and displacement field of a wetted material. The method is applied here in monitoring the wetting-swelling behaviour of bentonite clay samples enclosed in a sample chamber of constant total volume.

## Methods

### *X-ray tomography*

With X-ray tomography, the spatial distribution of the linear X-ray attenuation coefficient (LAC) in the sample is obtained [13]. In a typical X-ray tomographic imaging procedure, of the order of one thousand X-ray projection images of the sample are taken from different directions by rotating the sample in the X-ray beam. The three-dimensional distribution of LAC is then reconstructed from the projection images by a computer. The data is conveniently represented as a three-dimensional gray-scale image (stack of two-dimensional cross-sectional images) allowing not only visualization but also quantitative study of the internal structure of many heterogeneous materials. The gray-scale 'voxel' values in such an image are linearly correlated with the actual LAC value in the sample. In a case of monochromatic X-ray beam, the gray-scale value (or the LAC) is furthermore linearly correlated with partial densities of materials present in the sample so for the solid-liquid system the gray-scale value is

$$G = C + \alpha_s \cdot \rho_s + \alpha_l \cdot \rho_l \quad (1)$$

where  $C$ ,  $\alpha_s$  and  $\alpha_l$  are constants depending on materials and settings used. For a polychromatic X-ray source (*e.g.* X-ray tube), linearity in Eq. 1 may not hold exactly due to beam hardening artifact. However, this artifact can be corrected at the reconstruction stage which seems to work well for the purposes of this study. There are usually many other artifacts present in images such as ring artifacts, cone-beam artifacts and noise. Those can be reduced by optimizing scanning settings or performing specific corrections in reconstruction software.

The X-ray microtomographic device used in the present work was SkyScan 1172 desktop scanner (Fig. 1) which has a microfocus X-ray tube with maximum operating voltage of 100 kV and maximum power of 10 W. The minimum pixel size is 0.7  $\mu\text{m}$  but for the purposes of the present study the device was used in a reduced resolution mode with image size 1000 x 524 pixels of size 24  $\mu\text{m}$ .

### *Experimental set-up and samples*

Cylindrical bentonite samples of diameter 17 mm and height 10 mm were made by compacting a weighed amount of bentonite powder (MP Biomedicals Bentonite) in a mould into a predetermined mean solid phase partial density (1.2 – 1.5  $\text{g}/\text{cm}^3$ ), and placed in a sample holder (see Fig. 1). In order to facilitate deformation measurement, hollow glass microspheres of diameter 100  $\mu\text{m}$  were mixed with the bentonite powder to act as inert tracer particles in the otherwise quite homogeneous material. During the experiment, the sample was held in approximately constant volume in a plastic (PEEK) tube and between cylindrical end-pieces. The end-pieces include wetting and venting channels, and glass sintered plates that allow liquid flow in the sample through the lower end surface, and escape of air through the upper surface. The experiment was started by taking a reference state tomographic image of the non-wetted sample and after that, the wetting (simulated groundwater) of the sample was initiated. The wetting was periodically interrupted and the sample holder with the partially saturated sample weighed, scanned in the tomographic device, weighed again and reconnected to liquid supply to resume wetting. The scanning time was about 45 minutes, and the total time required for each scanning-weighing interval was about an hour. The procedure was repeated typically 10 times until the sample was completely saturated in about 1–2 weeks total time.

### *Deformation analysis*

The local displacement of the solid phase caused by swelling can, in principle, be found by comparing the tomographic images of the reference state and each of the partially wetted states of the sample, provided that both images contain enough tractable details. The displacement

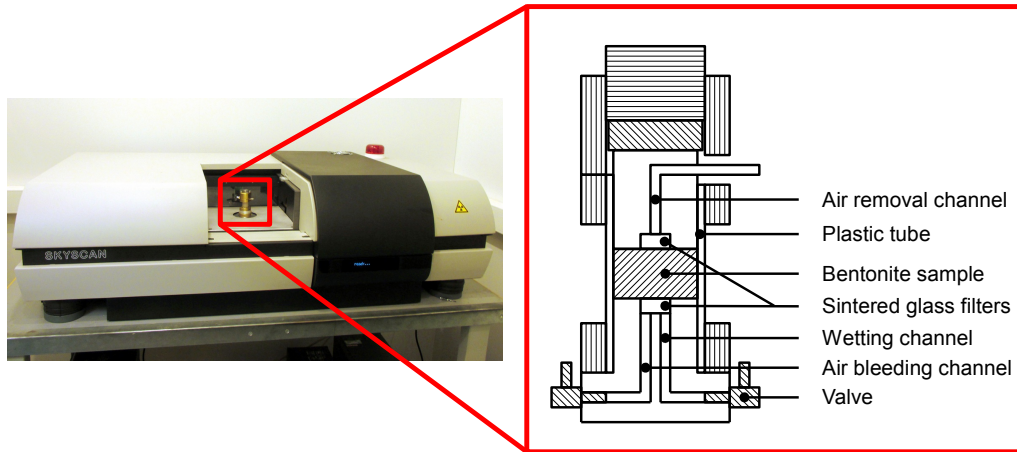


Figure 1. Microtomographic device (SkyScan 1172) and schematic cross-sectional view of the sample holder.

vectors are determined in a three-dimensional grid defined in the reference state image. At every point of that grid, a reference subimage is compared with subimages extracted from the deformed image at the vicinity of the grid point. The minimum for the sum of the squares of the difference in voxel values then defines the measured displacement for that particular grid point. Sub-pixel accuracy is further achieved by fitting second order polynomial function to the minimum.

In order to test the deformation analysis algorithm, a cylindrical sample was made of two-component liquid rubber material doped with glass tracer particles similarly to the bentonite samples. The rubber sample was placed in a material testing stage that allows tomographic imaging of the material under compression or tension. A reference tomographic image of the sample was taken at zero load. The sample was then compressed axially inducing deformation into a barrel-like shape, and imaged again in this configuration. The subimage matching algorithm was used to calculate the displacement field between the unloaded reference state and the deformed state. The experimental result was compared with a numerical solution for the same set-up obtained by COMSOL software indicating very close qualitative and quantitative agreement.

#### *Liquid content distribution*

The unknown coefficients ( $C$ ,  $\alpha_s$  and  $\alpha_l$ ) in the Eq. 1 can be evaluated from measurements of additional calibration samples made by varying solid and liquid densities. The reference tomographic image gives the initial density of the solid material if the possible liquid content in the reference state is known (measurable and assumed to be constant here). The change in solid density between wetted and reference state can be calculated from the measured displacement field and therefore the solid density distribution is known in the wetted state. The remaining unknown quantity, *i.e.* the liquid density  $\rho_l$  can then be calculated from in Eq. 1.

The tomographic liquid content analysis method discussed above was compared with results from a straightforward gravimetric analysis of subsamples obtained by slicing a partially wetted (22 h) test sample. After CT method, the sample was carefully cut horizontally into 10 slices of thickness about 1 mm. The liquid content of each slice was determined gravimetrically using oven drying at 105 °C. The results obtained from the gravimetric measurement and from the tomographic imaging method indicate reasonably good correspondence between the two results in regions well inside the sample.

## Results

The X-ray tomographic imaging and image analysis methods described above yield three-dimensional displacement field and liquid content distributions in the material sample at selected times during the slow wetting process. Typical examples of such results averaged over the azimuthal angle for a bentonite sample wetted in the sample holder chamber are visualized in Fig. 2. The results on displacement distributions obtained by the X-ray tomographic analysis appear consistent and repeatable in the entire sample region. The water transport mechanism resembles diffusion which is characteristic for the bentonite. The time evolution of the displacement field seems to be complicated which indicates that the swelling of the bentonite is complex phenomenon.

The most important source of error in the deformation analysis are the spurious displacement vector values that occasionally appear as a result of false local minima found by the image correlation algorithm. Those do not seem to have significant contribution to azimuthally averaged results. Another experimental issue affecting the accuracy of liquid content measurement is the incomplete stability of the X-ray source and detector. For accurate results, very good stability is required during each individual scan and between the scans during the experiment. Although, lacking an applicable reference method, quantitative assessment of absolute errors of both the local displacement and the total local liquid content analysis is not feasible, the overall confidence level of the results is reflected by the deformation and wetting test cases.

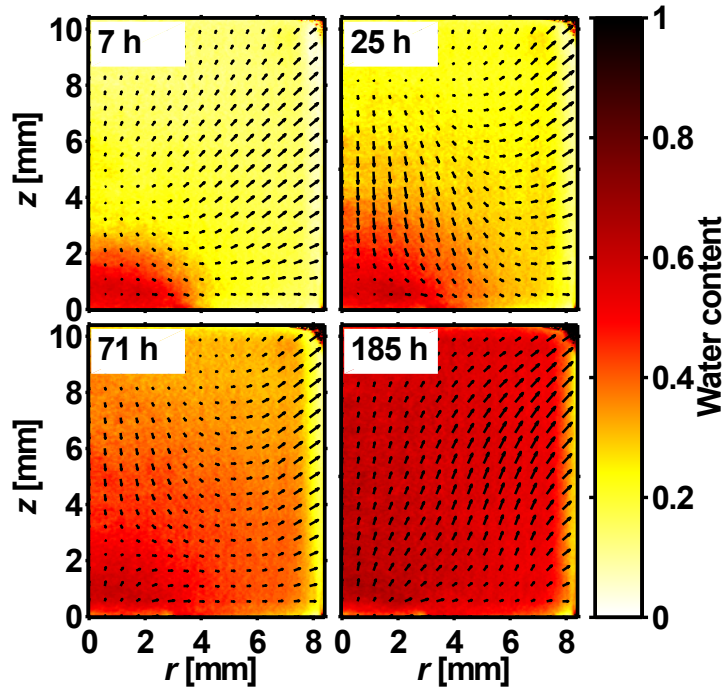


Figure 2. Azimuthally averaged displacement field (scaled by a factor of 5) and water content ( $\rho_l/\rho_s$ ) in a bentonite sample measured at four different times during wetting.

## Conclusions

A method for simultaneous non-intrusive analysis of three-dimensional deformation and liquid transport in solid, wetting material, based on X-ray tomographic imaging has been introduced. The analysis is based on comparing the tomographic images of the reference state and of a wetted and deformed state. The displacement field is obtained by a straightforward image correlation method. This requires that a sufficient amount of local detail, identifiable in the two images, are

found in both states, and that the imaging resolution is sufficient for revealing the deformations. In addition, liquid transport in the material should be slow enough such that the sample can be considered approximately stationary during a single tomographic scan. The deformation analysis was successfully compared with numerical solution for a rubber test sample under axial compression. The liquid content analysis was compared with gravimetric results from axially wetted and sliced cylindrical bentonite samples. The results showed relatively good accuracy in the interior parts of the sample. The method requires calibration with samples of known solid and liquid partial densities. The plausible sources of errors in the method are related to conical X-ray beam geometry, false displacements found by deformation analysis algorithm and instabilities in tomographic device. While the primary motivation and field of application in this work has been the study of the hydromechanical properties and swelling of bentonite clay, the developed method is potentially applicable in also other materials and processes involving liquid transport and deformation.

## References

- [1] P. Moldrup, T. Olesen, T. Komatsu, P. Schjønning, and D. E. Rolston. Tortuosity, diffusivity, and permeability in the soil liquid and gaseous phases. *Soil Science Society of America Journal*, 65(3):613–623, 2001.
- [2] J. Carmeliet and S. Roels. Determination of the isothermal moisture transport properties of porous building materials. *Journal of Building Physics*, 24(3):183–210, 2001.
- [3] I. S. Saguy, A. Marabi, and R. Wallach. New approach to model rehydration of dry food particulates utilizing principles of liquid transport in porous media. *Trends in Food Science & Technology*, 16(11):495–506, 2005.
- [4] F. C. Meinzer. Co-ordination of vapour and liquid phase water transport properties in plants. *Plant, Cell & Environment*, 25(2):265–274, 2002.
- [5] C. M. K. Gardner, D. Robinson, K. Blyth, and J. D. Cooper. *Soil water content. In Soil and environmental analysis: Physical methods.* CRC Press, 2000.
- [6] J.-J. Orteu. 3-D computer vision in experimental mechanics. *Optics and Lasers in Engineering*, 47(3):282–291, 2009.
- [7] K.-H. Herrmann, A. Pohlmeier, D. Gembris, and H. Vereecken. Three-dimensional imaging of pore water diffusion and motion in porous media by nuclear magnetic resonance imaging. *Journal of Hydrology*, 267(3):244–257, 2002.
- [8] W. Aregawi, T. Defraeye, S. Saneinejad, P. Vontobel, E. Lehmann, J. Carmeliet, D. Derome, P. Verboven and B. Nicolai. Dehydration of apple tissue: Intercomparison of neutron tomography with numerical modelling. *International Journal of Heat and Mass Transfer*, 67:173–182, 2013.
- [9] M. Mukhlisin, A. Saputra, A. El-Shafie, and M. R. Taha. Measurement of dynamic soil water content based on electrochemical capacitance tomography. *International Journal of Electrochemical Science*, 7(6), 2012.
- [10] J. A. Huisman, S. S. Hubbard, J. D. Redman, and A. P. Annan. Measuring soil water content with ground penetrating radar. *Vadose zone journal*, 2(4):476–491, 2003.
- [11] S. Peth, J. Nellesen, G. Fischer, and R. Horn. Non-invasive 3D analysis of local soil deformation under mechanical and hydraulic stresses by  $\mu$ CT and digital image correlation. *Soil and Tillage Research*, 111(1):3–18, 2010.

- [12] H. Bart-Smith, A.-F. Bastawros, D. R. Mumm, A. G. Evans, D. J. Sypeck, and H. N. G. Wadley. Compressive deformation and yielding mechanisms in cellular Al alloys determined using X-ray tomography and surface strain mapping. *Acta Materialia*, 46(10):3583–3592, 1998.
- [13] S. R. Stock. *Microcomputed tomography: methodology and applications*. CRC press, 2008.